Physical Model Approach in the Study of the Transport of Alkyl Amines Across a Silicone Rubber Membrane in a Two-Chamber Diffusion Cell

DINESH C. PATEL, JEFFREY L. FOX, and WILLIAM I. HIGUCHI *x

Received December 22, 1978, from the *College of Pharmacy, The University of Michigan, Ann Arbor, MI 48109.* Accepted for publication July 26, 1983. *Present address: Department of Pharmaceutics, College of Pharmacy, The University of Utah, Salt Lake City, UT 84112.

Abstract □ The transport of hexylamine and octylamine through a silicone rubber membrane was studied as a function of buffer (phosphate) concentration and pH. The results were interpreted using a physical model which assumed a steady-state rate of transport and which accounted for (*a*) the simultaneous diffusion and rapid equilibrium of all the aqueous species, (*b*) the possible diffusion of both the amine and its protonated form through the membrane, and (*c*) the effect of a stagnant aqueous diffusion layer on each side of the membrane. The following conclusions were reached: (*a*) The thickness of the aqueous diffusion layer is ~100 μm, which is about the same as that previously measured for benzoic acid in this system. Transport of octylamine at pH ≥ 10 is ~90% aqueous diffusion layer controlled, whereas hexylamine is ~50% aqueous diffusion layer controlled at high pH. (*b*) The membrane permeability of octylamine is ~15–20 times that of hexylamine. This gives an incremental π constant for the partition coefficient of ~0.61, as compared with the previously reported value of 0.56. (*c*) At low pH (≤5), the transport of the protonated species becomes important. The membrane permeabilities of these ammonium ions are about four or five orders of magnitude less than the membrane permeabilities of the corresponding amines. The membranes were examined at 30,000× with the scanning electron microscope, and no evidence of holes was found.

Keyphrases □ Diffusion—transport of alkyl amines across a silicone rubber membrane □ Hexylamine—transport across a silicone rubber membrane, octylamine, two-chamber diffusion cell □ Octylamine—transport across a silicone rubber membrane, hexylamine, two-chamber diffusion cell

There is a need for an experimental system in which the transport of weak organic acids and bases across a lipoidal membrane can be studied. There are many situations in biopharmaceutics and therapeutics, including situations involving binding of drugs to macromolecules and micelles, in which such a system would be useful. Stehle and Higuchi (1, 2) have conducted studies on the transport of weak acids and bases across lipoidal membranes; however, these were of a limited nature. They used fiberglass filter disks preloaded with oil-polymer mixtures as lipoidal membranes. These membranes were not entirely satisfactory, as experiments could not be performed in the totally diffusion-controlled region. Also, membrane permeability changes with time were found in some of the experiments which were attributed to changes in the lipid viscosity with time.

Accordingly, this investigation was carried out to develop a rugged experimental system for studying the transport of weak acids and bases across lipoidal membranes and, simultaneously, to develop theoretical methods for analyzing the experimental results on a quantitative basis. We selected a silicone rubber membrane as our model membrane, as several investigators (3–8) have found it suitable for studying drug transport, and employed a standard two-chamber diffusion cell. This membrane may be used in consecutive experiments without significant changes in its permeability characteristics. We modified and adopted the theoretical relationships developed previously by Stehle and Higuchi (1, 2) and Suzuki *et al.* (9, 10) and show how this experimental system and the theoretical relationships can be productively employed in evaluation of pH, buffer concentration, and chain-length effects on the transport of weak bases from aqueous solutions across lipoidal membranes.

It is hoped that the results of these studies can also be used for quantitative determination of macromolecular binding or micellar solubilization of weak acids and bases in aqueous media. It can be argued that, where possible, the use of a lipoidal membrane would be preferred over the cellulose dialysis membrane for studying micellar solubilization of weak acids and bases because of the Donnan membrane effects encountered with cellophane membrane dialysis methods. Also, we hope to use this technique in the study of species distribution and the mechanisms of action of the amine-type cholesterol dissolution rate accelerators (11) in bile.

THEORETICAL SECTION

A physical model approach was utilized to study the transport of hexylamine and octylamine through a silicone rubber membrane as a function of buffer (phosphate) concentration and pH. The model used in this study is very similar to the one developed by Stehle and Higuchi (1, 2), in which a membrane separates two aqueous compartments, with an aqueous diffusion layer on each side of the membrane.

The steady-state model for amine, RN, which is protonated to RNH^+ at lower pH values, is illustrated in Fig. 1. Steady-state diffusion is assumed between donor and receiver compartments, and all relevant equilibria (the various phosphate species, as well as the free and protonated amines) are accounted for. The model allows for diffusion of protonated amine, as well as free amine, through the membrane.

The following equations describe the model under steady-state conditions. G, the total flux of the amine species RN and RNH^+ through each barrier, I–III, is given by:

$$GI = \{D_{RN}[(RN)_L - (RN)_1] + D_{RNH^+}[(RNH^+)_L - (RNH^+)_1]\}/h_1 \quad \text{(Eq. 1)}$$

$$GII = \{P_{RN}[(RN)_1 - (RN)_2] + P_{RNH^+}[(RNH^+)_1 - (RNH^+)_2]\}/h_2 \quad \text{(Eq. 2)}$$

$$GIII = \{D_{RN}[(RN)_2 - (RN)_R)] + D_{RNH^+}[(RNH^+)_2 - (RNH^+)_R]\}/h_3 \quad \text{(Eq. 3)}$$

where the subscripts 1 and 2 indicate the left and right aqueous interfacial locations, respectively, and subscripts L and R refer to the borders of left and right bulk aqueous phases, respectively (Fig. 1). D_{RN} and D_{RNH^+} (cm^2/s) are the aqueous diffusion coefficients of RN and RNH^+, respectively; P_{RN} and P_{RNH^+} are the membrane permeabilities (defined as the product of partition coefficient and diffusion coefficient) of RN and RNH^+, respectively; h_1 and h_3 (cm) are the effective thicknesses of the unstirred aqueous diffusion layers; h_2 is the membrane thickness. G is expressed in $mmol/cm^2 \cdot s$. At steady state, $GI = GII = GIII$.

Since it is assumed that no buffer species can penetrate the lipid phase, the total net flux of the buffer species through each of the two aqueous diffusion layers is zero at steady state. Hence, the equations for J_B, the total net flux of buffer species in the aqueous barriers, can be written as follows:

$$J_{BI} = D_{H_3PO_4}[(H_3PO_4)_L - (H_3PO_4)_1] + D_{H_2PO_4}[(H_2PO_4)_L - (H_2PO_4)_1] + D_{HPO_4}[(HPO_4)_L - (HPO_4)_1] + D_{PO_4}[(PO_4)_L - (PO_4)_1] = 0 \quad \text{(Eq. 4)}$$

0022-3549/84/0800-1028$01.00/0

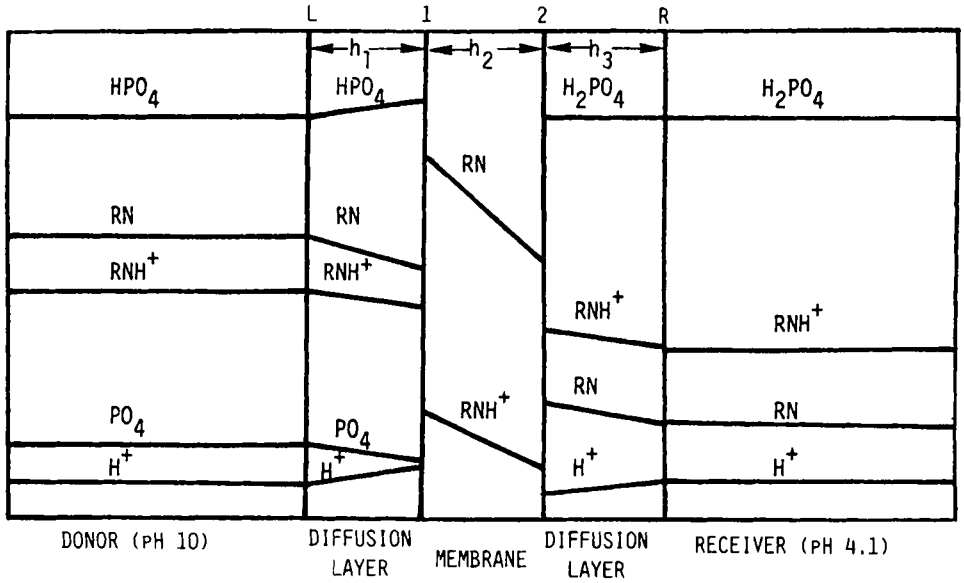

Figure 1—*Three-phase model showing schematic concentration profiles present in steady-state transport of amine, RN. RNH^+ is protonated amine; H_2PO_4, HPO_4, and PO_4 are buffer species (only the predominant species are shown in Fig. 1), and H^+ is hydrogen ion. h_1, h_2, and h_3 are diffusion barrier thicknesses in the three phases.*

$$J_B III = D_{H_3PO_4}[(H_3PO_4)_2 - (H_3PO_4)_R] + D_{H_2PO_4}[(H_2PO_4)_2 - (H_2PO_4)_R] + D_{HPO_4}[(HPO_4)_2 - (HPO_4)_R] + D_{PO_4}[(PO_4)_2 - (PO_4)_R] = 0 \quad \text{(Eq. 5)}$$

J_H, the net flux of H^+ minus the flux of OH^-, occurs *via* the transport of the protonated form of the amine, RNH^+, through the membrane and *via* the transport of all protonated species and also OH^- through the aqueous diffusion layers. The expressions for this quantity are given by:

$$J_{H^+}I = \{D_{RNH^+}[(RNH^+)_L - (RNH^+)_1] + 3D_{H_3PO_4}[(H_3PO_4)_L - (H_3PO_4)_1] + 2D_{H_2PO_4}[(H_2PO_4)_L - (H_2PO_4)_1] + D_{HPO_4}[(HPO_4)_L - (HPO_4)_1] + D_H[(H)_L - (H)_1] - D_{OH}[(OH)_L - (OH)_1]\}/h_1 \quad \text{(Eq. 6)}$$

$$J_{H^+}II = \{P_{RNH^+}[(RNH^+)_1 - (RNH^+)_2]\}/h_2 \quad \text{(Eq. 7)}$$

$$J_{H^+}III = \{D_{RNH^+}[(RNH^+)_2 - (RNH^+)_R] + 3D_{H_3PO_4}[(H_3PO_4)_2 - (H_3PO_4)_R] + 2D_{H_2PO_4}[(H_2PO_4)_2 - (H_2PO_4)_R] + D_{HPO_4}[(HPO_4)_2 - (HPO_4)_R] + D_H[(H)_2 - (H)_R] - D_{OH}[(OH)_2 - (OH)_R]\}/h_3 \quad \text{(Eq. 8)}$$

Analogous to the total amine flux, at steady state $J_HI = J_HII = J_HIII$. In the above equations, $D_{H_3PO_4}$, $D_{H_2PO_4}$, D_{HPO_4}, and D_{PO_4} (cm^2/s) are the aqueous diffusion coefficients of the H_3PO_4, H_2PO_4, HPO_4, and PO_4 buffer species, respectively, and D_H and D_{OH} (cm^2/s) are the aqueous diffusion coefficients of the hydrogen and hydroxyl ions, respectively.

In addition to satisfying the flux relationships expressed in Eqs. 1–8, a valid solution of the model must also satisfy all the chemical equilibrium constraints at each point in the system. These constraints can be written as follows (for n = 1, 2, L, R):

$$(HPO_4)_n = \frac{(H)_n(PO_4)_n}{K_{HPO_4}} \quad \text{(Eq. 9)}$$

$$(H_2PO_4)_n = \frac{(H)_n^2(PO_4)2_n}{K_{H_2PO_4}} \quad \text{(Eq. 10)}$$

$$(H_3PO_4)_n = \frac{(H)_n^3(PO_4)_n}{K_{H_3PO_4}} \quad \text{(Eq. 11)}$$

where $K_{HPO_4} = K_3$, $K_{H_2PO_4} = K_3 \cdot K_2$, and $K_{H_3PO_4} = K_3 \cdot K_2 \cdot K_1$ (K_1, K_2, and K_3 are the dissociation constants of phosphoric acid).

Similarly, for the amine (for n = 1, 2, L, R):

$$K_a = \frac{(RN)_n(H)_n}{(RNH^+)_n} \quad \text{(Eq. 12)}$$

where K_a is the dissociation constant of the protonated amine.

Given these relationships, the model can be used to calculate concentrations and fluxes of all the species at each point in the system when only the compositions of the bulk solutions on each side are given. This calculation is complicated by both the complex equilibria involved and the fact that a solution is sought for a system employing a trilaminar membrane. Nonetheless, the equations can be arranged in such a way that they can be rapidly solved with a digital computer if a program is available for the solution of systems of nonlinear algebraic equations. This particular problem can be reduced to a system of two equations in two unknowns by a number of different approaches. The algebraic approach employed here was to choose pH_1 and pH_2 (the pH values at the membrane surfaces) as the unknowns and, for a given set of values for pH_1 and pH_2, to calculate all the other quantities in such a way that all the problem constraints are satisfied, except for the constraint that $GI = GII = GIII$ at steady state. The nonlinear system solver then determines the values for pH_1 and pH_2 such that the equations $GI = GII$ and $GII = GIII$ are satisfied.

The algebraic procedure for calculating the species concentrations throughout the system for a given trial set of pH_1 and pH_2 values is as follows. First, the concentrations of all the species in the bulk solutions on each side of the membrane are calculated (for n = L, R):

$$(H)_n = 10^{-pH_n} \quad \text{(Eq. 13)}$$

$$(PO_4)_n = P_{tot_n} \Big/ \left(1 + \frac{(H)_n}{K_{HPO_4}} + \frac{(H)_n^2}{K_{H_2PO_4}} + \frac{(H)_n^3}{K_{H_3PO_4}}\right) \quad \text{(Eq. 14)}$$

$$(RN)_n = R_{tot_n} \Big/ \left(1 + \frac{(H)_n}{K_a}\right) \quad \text{(Eq. 15)}$$

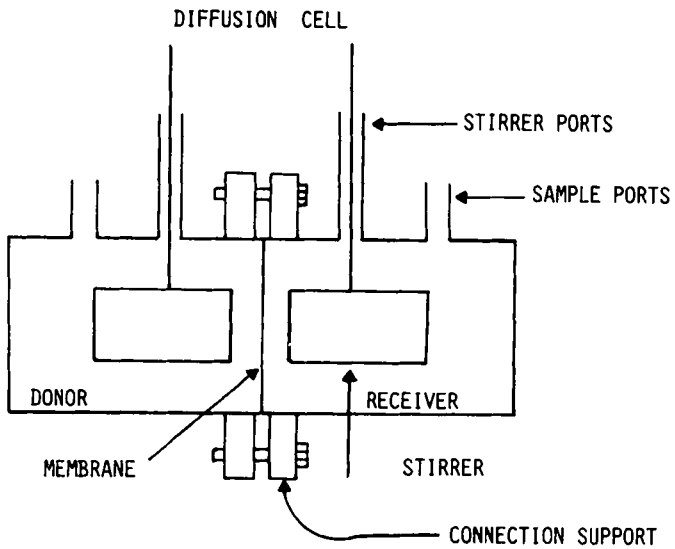

Figure 2—*Two-chamber diffusion cell used in transport studies. At predetermined intervals, donor and receiver solutions were totally replaced for analysis. Cross-sectional transport area was 2.10 cm^2.*

Table I—Typical Permeation Data [a]

Δ Time, h	Concentration, μg/mL Receiver	Donor	Flux, mmol/cm²·s [b]
0	0	546	—
2	9.9	514	5.654×10^{-11}
2	11.5	522	6.606×10^{-11}
2	13.2	519	7.562×10^{-11}
2	12.9	530	7.425×10^{-11}

[a] The system consisted of donor, 5 mM hexylamine, 0.1 M NaCl, and 0.1 M PO_4 (pH 8.5); receiver, 0.1 M NaCl and 0.1 M PO_4 (pH 4.1). [b] From the receiver data.

where P_{tot} and R_{tot} are total concentrations of the phosphate and amine, respectively. The concentrations of the other species can be readily calculated from $(H)_n$, $(PO_4)_n$, and $(RN)_n$ with Eqs. 9-12.

Next, the concentrations of the phosphate species at the membrane interfaces can be calculated by a suitable rearrangement of Eqs. 4 and 5 with appropriate substitutions from Eqs. 9-11. The concentrations of PO_4 at the interfaces are given by:

$$(PO_4)_1 = [D_{H_3PO_4}(H_3PO_4)_L + D_{H_2PO_4}(H_2PO_4)_L + D_{HPO_4}(HPO_4)_L + D_{PO_4}(PO_4)_L] \Big/ \left[D_{H_3PO_4}\frac{(H)_1^3}{K_{H_3PO_4}} + D_{H_2PO_4}\frac{(H)_1^2}{K_{H_2PO_4}} + D_{HPO_4}\frac{(H)_1}{K_{HPO_4}} + D_{PO_4}\right] \quad \text{(Eq. 16)}$$

and:

$$(PO_4)_2 = [D_{H_3PO_4}(H_3PO_4)_R + D_{H_2PO_4}(H_2PO_4)_R + D_{HPO_4}(HPO_4)_R + D_{PO_4}(PO_4)_R] \Big/ \left[D_{H_3PO_4}\frac{(H)_2^3}{K_{H_3PO_4}} + D_{H_2PO_4}\frac{(H)_2^2}{K_{H_2PO_4}} + D_{HPO_4}\frac{(H)_2}{K_{HPO_4}} + D_{PO_4}\right] \quad \text{(Eq. 17)}$$

and the concentrations of HPO_4, H_2PO_4, and H_3PO_4 follow from Eqs. 9-11.

Thus far, for given values of pH_1 and pH_2 we have determined concentrations of the various phosphate species at 1 and 2 so that the net total phosphate flux is zero. The remaining task is to determine the concentrations of RN and RNH^+ at these interfaces that satisfy the equations for total proton flux (Eqs. 6-8). This task is greatly facilitated by defining new variables *RI* and *RIII* such that:

$$RI = J_H I + \frac{D_{RNH^+}}{h_1}(RNH^+)_1 \quad \text{(Eq. 18)}$$

and

$$RIII = J_H III - \frac{D_{RNH^+}}{h_3}(RNH^+)_2 \quad \text{(Eq. 19)}$$

Table II—Model Parameters [a]

Parameter	Known	Computer Fitted
D_{OH}	5×10^{-5} cm²/s	
D_H	9×10^{-5} cm²/s	
D_{RN}, D_{RNH^+} (hexylamine)	1.087×10^{-5} cm²/s	
D_{RN}, D_{RNH^+} (octylamine)	9.880×10^{-6} cm²/s	
$D_{H_3PO_4}$, $D_{H_2PO_4}$, D_{HPO_4}, kD_{PO_4},	10^{-5} cm²/s	
h_1 and h_3	0.009 cm	0.01 cm
h_2	0.0127 cm	
K_1 (H_3PO_4)	7.50×10^{-3}	
K_2 (H_3PO_4)	6.20×10^{-8}	
K_3 (H_3PO_4)	2.10×10^{-13}	
K_a (hexylamine)	2.7542×10^{-11}	
K_a (octylamine)	2.2387×10^{-11}	
P_{RN} (hexylamine)		2.27×10^{-5} cm²/s
P_{RNH^+} (hexylamine)		4.130×10^{-9} cm²/s
P_{RN} (octylamine)		3.88×10^{-4} cm²/s
P_{RNH^+} (octylamine)		3.770×10^{-9} cm²/s

[a] Diffusivities for hexylamine and octylamine were determined experimentally; those for hydrogen and hydroxyl ions were calculated from mobility data. For the phosphate species, we assumed 10^{-5} cm²/s to be a reasonable estimate based on previous experience.

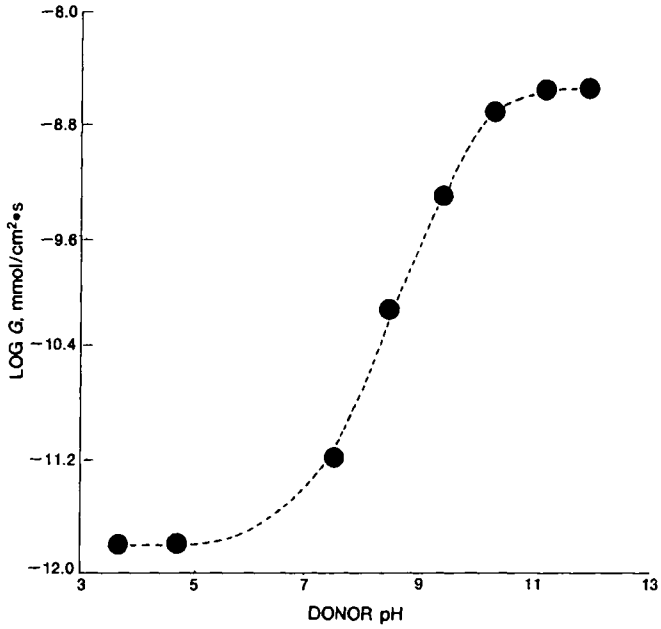

Figure 3—*pH-rate profile for hexylamine diffusing through the silicone rubber membrane into aqueous phase buffered at pH 4.1. The dashed line is a computer-generated line for* $h_1 = h_3 = 100$ *μm,* $h_2 = 127$ *μm,* $P_{RN} = 2.27 \times 10^{-5}$ *cm²/s, and* $P_{RNH^+} = 4.13 \times 10^{-9}$ *cm²/s.*

Numerical values for *RI* and *RIII* are readily obtained by substituting Eqs. 18 and 19 into Eqs. 6 and 8 and rearranging to get:

$$h_1 \cdot RI = D_{RNH^+}(RNH^+)_L + D_H[(H)_L - (H)_1] + D_{HPO_4}\left[(HPO_4)_L - \frac{(H)_1(P)_1}{K_{HPO_4}}\right] + 2D_{H_2PO_4}\left[(H_2PO_4)_L - \frac{(H)_1^2(PO_4)_1}{K_{H_2PO_4}}\right] + 3D_{H_3PO_4}\left[(H_3PO_4)_L - \frac{(H)_1^3(PO_4)_1}{K_{H_3PO_4}}\right] - D_{OH}[(OH)_L - (OH)_1] \quad \text{(Eq. 20)}$$

$$h_3 \cdot RIII = D_{RNH^+}(RNH^+)_R + D_H[(H)_R - (H)_2] + D_{HPO_4}\left[(HPO_4)_R - \frac{(H)_2(PO_4)_2}{K_{HPO_4}}\right] + 2D_{H_2PO_4}\left[(H_2PO_4)_R - \frac{(H)_2^2(PO_4)_2}{K_{H_2PO_4}}\right] + 3D_{H_3PO_4}\left[(H_3PO_4)_R - \frac{(H)_2^3(PO_4)_2}{K_{H_3PO_4}}\right] - D_{OH}[(OH)_R - (OH)_2] \quad \text{(Eq. 21)}$$

Consideration of Eqs. 6, 18, and 19 leads to:

$$h_2 \cdot h_1 \cdot RI = P_{RNH^+} \cdot h_1[(RNH^+)_1 - (RNH^+)_2] + h_2 \cdot D_{RNH^+}[RNH^+]_1 \quad \text{(Eq. 22)}$$

and

$$h_2 \cdot h_3 \cdot RIII = P_{RNH^+} \cdot h_3([RNH^+]_1 - [RNH^+]_2) - h_2 \cdot D_{RNH^+}[RNH^+]_2 \quad \text{(Eq. 23)}$$

or:

$$\begin{pmatrix} h_1 P_{RNH^+} \cdot h_2 D_{RNH^+} & -h_1 P_{RNH^+} \\ h_3 PRNH^+ & -h_3 P_{RNH^+} - h_2 D_{RNH^+} \end{pmatrix} \begin{pmatrix} [RNH^+]_1 \\ [RNH^+]_2 \end{pmatrix} = \begin{pmatrix} h_2 h_1 RI \\ h_2 h_3 RIII \end{pmatrix} \quad \text{(Eq. 24)}$$

Table III—Influence of the Aqueous Diffusion Layer

Donor pH	Receiver pH	Flux, mmol/cm²·s
	Hexylamine	
11.20	11.00	1.987×10^{-9}
11.20	4.10	2.975×10^{-9}
	Octylamine	
11.10	11.00	2.518×10^{-9}
11.10	4.10	4.951×10^{-9}

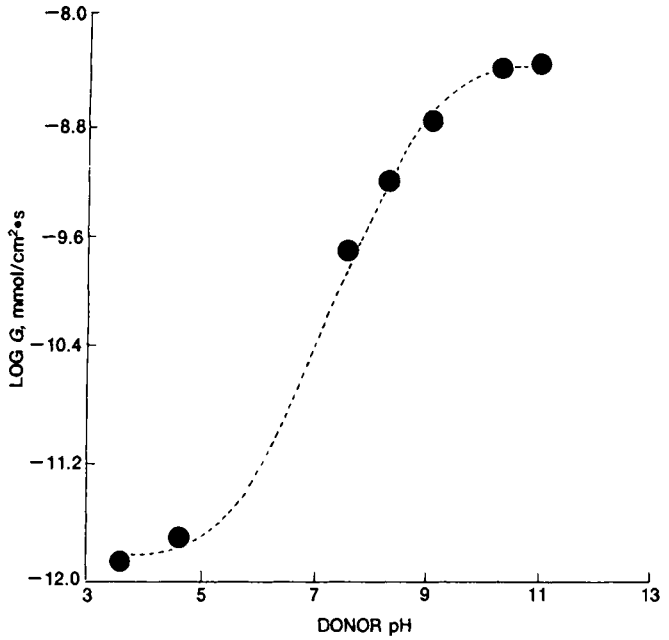

Figure 4—*pH-rate profile for octylamine diffusing through the silicone rubber membrane into aqueous phase buffered at pH 4.1. The dashed line is a computer-generated line for* $h_1 = h_3 = 100\ \mu m$, $h_2 = 127\ \mu m$, $P_{RN} = 3.88 \times 10^{-4}\ cm^2/s$, *and* $P_{RNH^+} = 3.77 \times 10^{-9}\ cm^2/s$.

where every quantity except $(RNH^+)_1$ and $(RNH^+)_2$ has been calculated. This equation is solved for $(RNH^+)_1$ and $(RNH^+)_2$, after which $(RN)_1$ and $(RN)_2$ are calculated from Eq. 12. Finally, *GI*, *GII*, and *GIII* are calculated from Eqs. 1-3 and the functions:

$$f_1 = GI - GII \qquad \text{(Eq. 25)}$$

and:

$$f_2 = GIII - GII \qquad \text{(Eq. 26)}$$

are evaluated. The procedure is repeated, with the nonlinear system solver adjusting the values of pH_1 and pH_2 until f_1 and f_2 are arbitrarily close to zero.

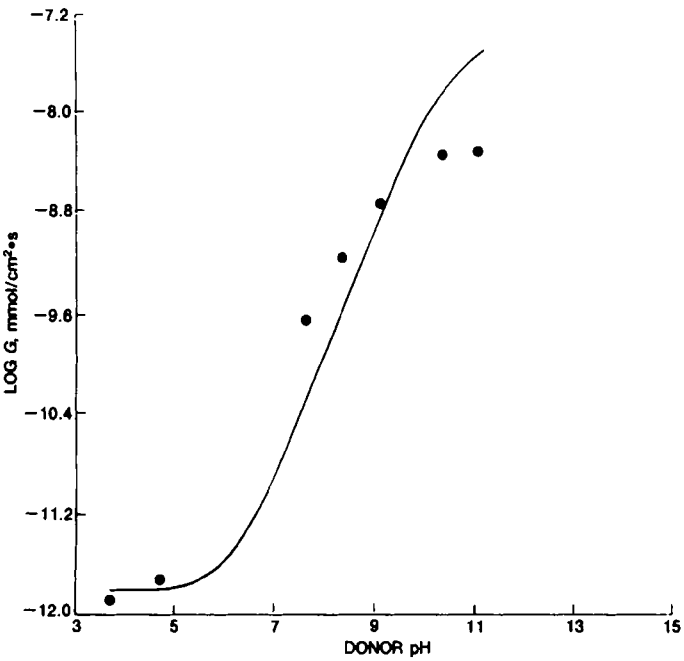

Figure 5—*pH-rate profile for octylamine diffusing through the silicone rubber membrane into aqueous phase buffered at pH 4.1. The solid line is a computer-generated line for* $h_1 = h_3 = 0\ \mu m$, $h_2 = 127\ \mu m$, $P_{RN} = 9.586 \times 10^{-5}\ cm^2/s$, *and* $P_{RNH^+} = 4.017 \times 10^{-9}\ cm^2/s$.

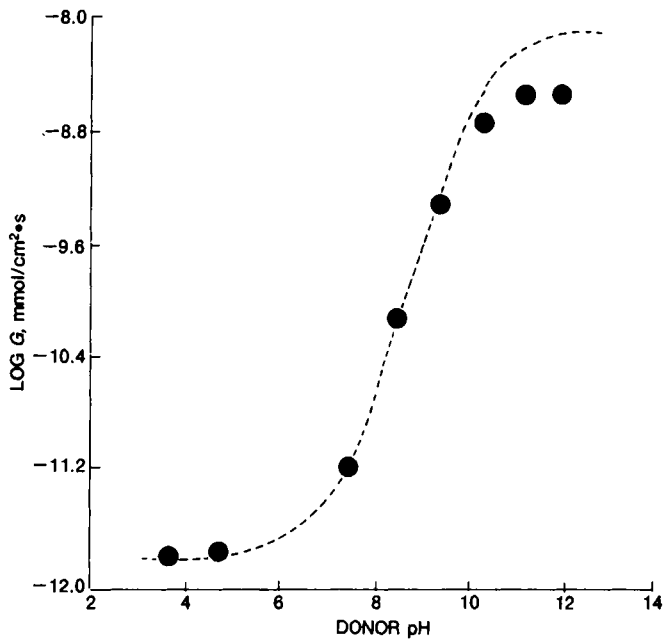

Figure 6—*pH-rate profile for hexylamine diffusing through the silicone rubber membrane into aqueous phase buffered at pH 4.1. The dashed line is a computer-generated line for* $h_1 = 0\ \mu m$, $h_2 = 127\ \mu m$, $h_3 = 100\ \mu m$, $P_{RN} = 2.27 \times 10^{-5}\ cm^2/s$, *and* $P_{RNH^+} = 4.13 \times 10^{-7}\ cm^2/s$.

EXPERIMENTAL SECTION

Experimental Design—The overall permeation procedure was designed such that depletion of the donor concentration was negligible during the course of the runs, and the receiver concentration was never an appreciable fraction of the donor concentration. Under these circumstances, the steady-state condition is readily attained.

The presence of the aqueous diffusion layer was studied by conducting studies in which the receiver compartment pH was maintained at pH 11.0 or 4.1. At high pH, the resistance of the aqueous diffusion layer causes a concentration gradient across the aqueous diffusion layer, and permeation of the weak base is reduced. At low pH, the aqueous diffusion layer is "short-circuited," *i.e.*, the aqueous diffusion layer offers no significant resistance to the transport of the weak base. When the aqueous diffusion layers are the main barriers for the weak base transport, elimination of half of the total aqueous diffusion layer resistance should result in ~100% increase in the permeation rate.

To study the influence of pH and buffer concentration on permeation, permeation was measured as a function of donor pH and donor buffer concentration. The pH of the donor compartment was closely monitored. The receiver compartment solution was buffered at pH 4.1 to ensure zero concentration of un-ionized drug; thus, perfect sink conditions were obtained.

Materials—*n*-Octylamine[1], *n*-hexylamine[2], sodium chloride[3], picric acid[4], dichloromethane[5], and sodium phosphate[5] (monobasic and dibasic) were reagent grade and used as received.

Preparation of Membrane—Membranes were cut from sheets of nonreinforced dimethylpolysiloxane[6], reportedly 0.127-cm thick, with a die made especially for the diffusion cell. Initially, they were washed in hot water, thoroughly rinsed with distilled water, and allowed to equilibrate overnight in receiver solution. Fresh membrane was used for each experiment.

Diffusion Cell—The diffusion cell consisted of two cylindrical half-cells, with inside diameters of ~1.5 cm and depths of ~5 cm. This gave a half-cell volume of ~9 mL. The cell halves were assembled, with the membrane between half-cells (Fig. 2), using polytef connection supports. The entire cell was immersed in a constant-temperature bath. The cell contents were stirred with small stirrers on shafts driven at 150 rpm by a constant-speed motor.

Permeation Procedure—Donor solution (9 mL) was placed in one half-cell, and 9 mL of receiver solution was placed in the other half-cell. The receiver solution consisted of 0.1 M NaCl and 0.1 M phosphate buffer. The donor

[1] Aldrich Chemical Co., Milwaukee, Wis.
[2] Eastman Kodak Co., Rochester, N.Y.
[3] Fisher Scientific Co., Fair Lawn, N.J.
[4] MCB, Norwood, Ohio.
[5] Mallinckrodt, St. Louis, Mo.
[6] Silastic; Dow Corning Corp., Midland, Mich.

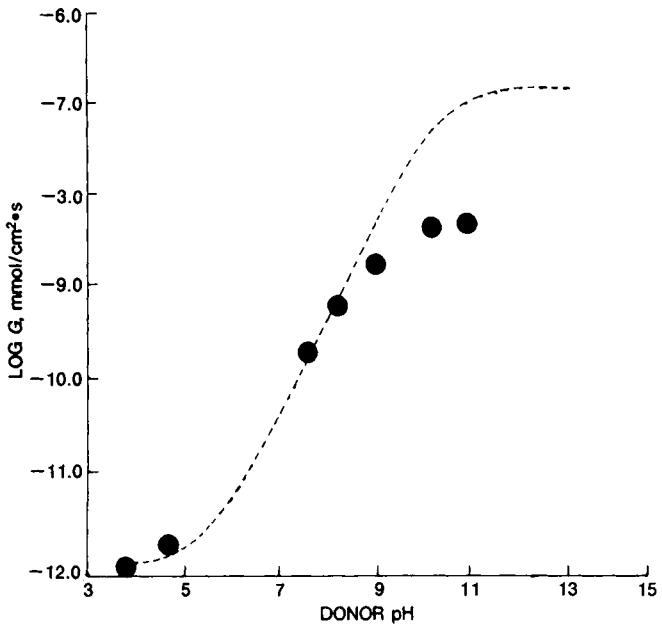

Figure 7—*pH-rate profile for octylamine diffusing through the silicone rubber membrane into aqueous phase buffered at pH 4.1. The dashed line is a computer-generated line for* $h_1 = 0$ *μm,* $h_2 = 127$ *μm,* $h_3 = 100$ *μm,* $P_{RN} = 3.88 \times 10^{-4}$ *cm²/s, and* $P_{RNH^+} = 3.77 \times 10^{-9}$ *cm²/s.*

solution consisted of the amine and 0.1 M NaCl in 0.1 M phosphate buffer. The contents of each half-cell were stirred at 150 rpm. At predetermined intervals, donor and receiver solutions were totally replaced for analysis. The total time involved in the exchange of the solutions was 1–2 min. The experiment was continued until the difference between two consecutive receiver compartment concentrations was <5%. The average of these concentrations was then used to calculate the flux under essentially steady-state conditions.

The amine analysis involved complexation of the amine with picric acid. The concentration of this picrate complex was determined spectrophotometrically. Receiver solution (5 mL) was shaken in a separatory funnel with two successive portions of 10 and 15 mL of a 0.2% solution of picric acid in dichloromethane. The two portions were drawn off, and the absorbance of these solutions was determined spectrophotometrically at a wavelength of 420 nm[7]. Picric acid was used as the reagent here for assaying the amines because it has a strong absorption spectrum and a single strong anionic functional group that has been shown to react quickly and quantitatively with the base (12, 13).

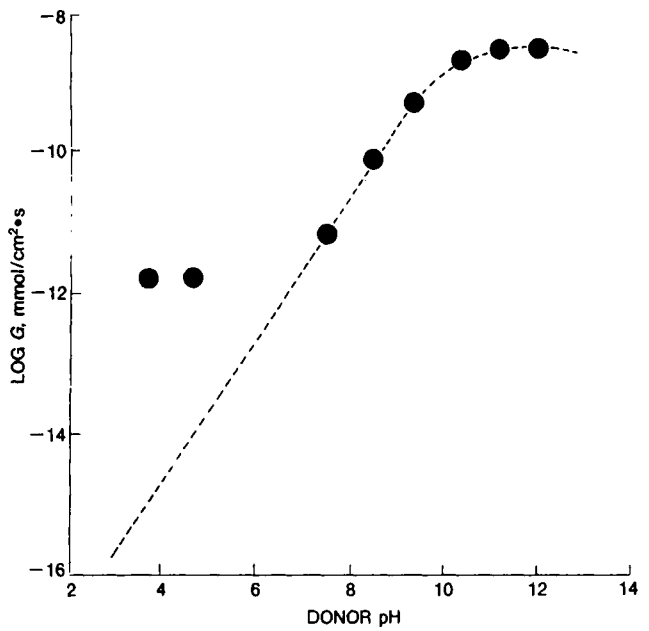

Figure 8—*pH-rate profile for hexylamine diffusing through the silicone rubber membrane into aqueous phase buffered at pH 4.1. The dashed line is a computer-generated line for* $h_1 = h_3 = 100$ *μm,* $h_2 = 127$ *μm,* $P_{RN} = 2.27 \times 10^{-5}$ *cm²/s, and* $P_{RNH^+} = 0$ *cm/2.*

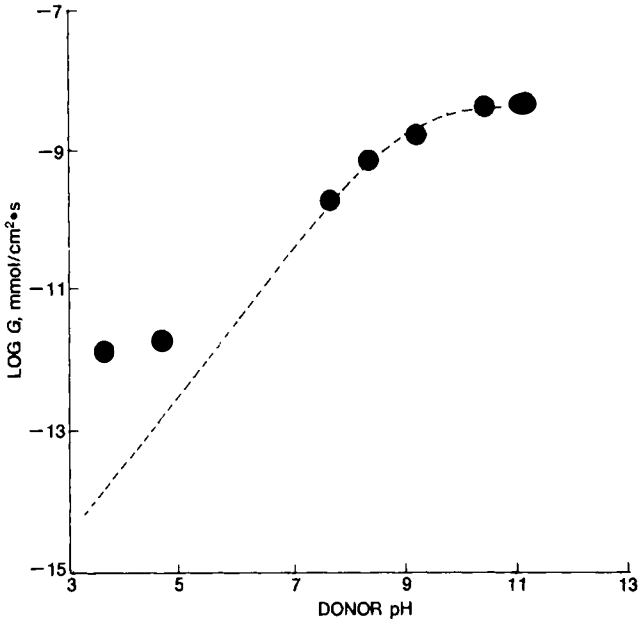

Figure 9—*pH-rate profile for octylamine diffusing through the silicone rubber membrane into aqueous phase buffered at pH 4.1. The dashed line is a computer-generated line for* $h_1 = h_3 = 100$ *μm,* $h_2 = 127$ *μm,* $P_{RN} = 3.88 \times 10^{-4}$ *cm²/s, and* $P_{RNH^+} = 0$ *cm²/s.*

Except at low pH (pH $\lesssim$ 6.0), the typical uncertainty in the flux determination was on the order of 5%. At low pH, because of the extremely low fluxes, the errors were relatively large (~25–50%).

RESULTS AND DISCUSSION

Table I shows typical transport data, from which it can be seen that a 5% error in the donor compartment would result in ~ ±26 μg/mL scatter; this scatter is greater than the amount transported across the membrane. Hence, it was decided to calculate the flux from the receiver compartment data only. Typically, steady-state conditions were attained within 2–4 h.

The initial steady-state flux into the receiver compartment is given by:

$$\text{Flux} = \frac{V}{A} \cdot \frac{dC}{dt} = k \cdot C_0 \text{ mmol/cm}^2 \cdot \text{s} \qquad \text{(Eq. 27)}$$

where V is the donor compartment volume, A is the diffusional area of the membrane, dC/dt is the rate at which drug permeates the membrane under steady-state conditions, C_0 is the concentration differential across the membrane (assumed to be initial donor concentration), and k is the permeability constant. Thus, k can be calculated from the experimental data by:

$$k = \frac{V \cdot \frac{dC}{dt}}{A \cdot C_0} \qquad \text{(Eq. 28)}$$

Variation in flux from run to run was 5–10% when the fluxes were $>10^{-11}$; for fluxes $<10^{-11}$ cm²/s, variation was 25–50%. Table II shows the values of various model parameters. Of the model parameters, the only unknown is the membrane permeability (defined as the partition coefficient multiplied by diffusivity) which is obtained by computer fitting (14).

Using nonlinear least-squares regression, best values were found for the membrane permeabilities and the aqueous diffusion layer thickness by the following technique. Trial values for the unknown parameters were assumed. Then, Eqs. 1–26 were solved, as described above, to calculate flux as a function of solution composition. The calculated values were compared with the experimentally observed fluxes, and the sum of the squares of the relative differences between calculated and observed fluxes was computed. Then, new values were chosen for the unknown parameters, and the procedure was re-

[7] Model 139, Hitachi Perkin-Elmer UV-V15 Spectrophotometer; Hitachi Ltd., Japan.

Table IV—Influence of Buffer Concentration on Hexylamine

Donor pH	Flux, mmol/cm²·s	
	0.1 M PO_4	0.01 M PO_4
12.05	3.334×10^{-9}	3.269×10^{-9}
9.50	5.210×10^{-10}	1.696×10^{-10}
7.50	7.154×10^{-12}	7.200×10^{-12}

peated. This entire cycle was repeated using a nonlinear least-squares fitting program until the sum of squares was minimized.

For both compounds, the diffusion layer thickness was found to be ~100 μm. The membrane permeabilities were as follows (cm²/s): free hexylamine, 2.27×10^{-5}; protonated hexylamine, 4.13×10^{-9}; free octylamine, 3.88×10^{-4}; protonated octylamine, 3.77×10^{-9}. Figures 3 and 4 show the experimental fluxes and theoretical fluxes based on parameter values shown in Table II. Over a range of more than 7 pH units and three orders of magnitude of flux, the model gives an essentially perfect fit to data.

Table III shows the influence of high and low pH in the receiver compartment on permeation. At low pH, the aqueous diffusion layer in the receiver compartment is essentially "short-circuited," *i.e.*, the effective transport resistance is very low. For octylamine under these conditions, this is an ~100% increase in flux, which indicates that the transport is essentially 100% aqueous diffusion layer controlled for this solute. However, for hexylamine, it can be seen that there is only an ~50% increase; this means that the membrane transport resistance is an appreciable part of the overall resistance in the case of hexylamine.

The thickness of the aqueous diffusion layer was independently evaluated by mounting a benzoic acid pellet onto the half-cell. The thickness was calculated from:

$$J/A = \frac{D(C_s - C_b)}{h} \qquad \text{(Eq. 29)}$$

where J is the dissolution rate (flux), A is the surface area of dissolving solid exposed to the solution, C_s is the concentration of the solute in the solution at saturation, C_b is the concentration of the solute in the bulk, D is the diffusion coefficient of the solute in the solvent (1.4×10^{-5} cm²/s at 37°C), and h is the Nernst effective diffusion layer thickness. Under sink conditions, $C_b = 0$; J/A and C_s were experimentally determined, and the value of D has been well documented previously (15). The thickness of the aqueous diffusion layer was found to be 90 μm. Hence, the computer-fit value of 100 μm is reasonable.

To determine whether the experimental data could fit a model in which there were no aqueous diffusion layers, *i.e.*, $h_1 = h_3 = 0$, best values were found for the membrane permeabilities using nonlinear least-squares regression and values listed in Table II, except for the membrane permeabilities and the aqueous diffusion layer thickness. Figure 5 shows the best fit when the aqueous diffusion layers are totally neglected. As can be seen under such circumstances, *i.e.*, when $h_1 = h_3 = 0$, the fit between the experimental values and the values predicted by the model is rather poor.

To assess the importance of the aqueous diffusion layers and the membrane permeabilities of the protonated species on the steady-state flux, computer simulations were made using the model parameters listed in Table II but excluding the parameter of interest. Figures 6 and 7 show that if the aqueous diffusion layer of the donor compartment is left out, the fluxes are significantly greater at the higher pH values. This shows that the aqueous diffusion layer is important, and significant errors in the analysis may result when it is ignored.

Figures 8 and 9 show the expected behavior if no protonated amine species were diffusing through the membrane. The theoretical fluxes were much smaller than the experimental fluxes at lower pH values. This clearly indicates that protonated amines are diffusing through the membrane, although they have much lower apparent membrane permeabilities than the free amines. These membranes were examined *via* scanning electron microscopy at 30,000×, and no evidence of holes was found, which supports the hypothesis of a true diffusion through the membrane of the protonated species.

Table IV shows the influence of buffer concentration on permeation. At pH values at which the buffer capacity is good (pH 12.05 and 7.50), the buffer concentration has no significant influence on permeation. At pH 9.5, at which the buffer capacity is poor, a lower flux was observed when the buffer strength was 0.01 M. This was the result of a drop in the bulk pH of ~1 pH unit at the lower buffer concentration, which was theoretically predicted and experimentally observed.

Figure 10 shows the effect of the alkylamine chain length. The membrane permeability of octylamine is 15–20 times that of hexylamine. If it is assumed that the membrane diffusivities of these two compounds are about equal, this leads to an incremental π constant for the partition coefficient per methylene group of ~0.61, which is in good agreement with the value of 0.56 reported by Flynn and Yalkowsky (16).

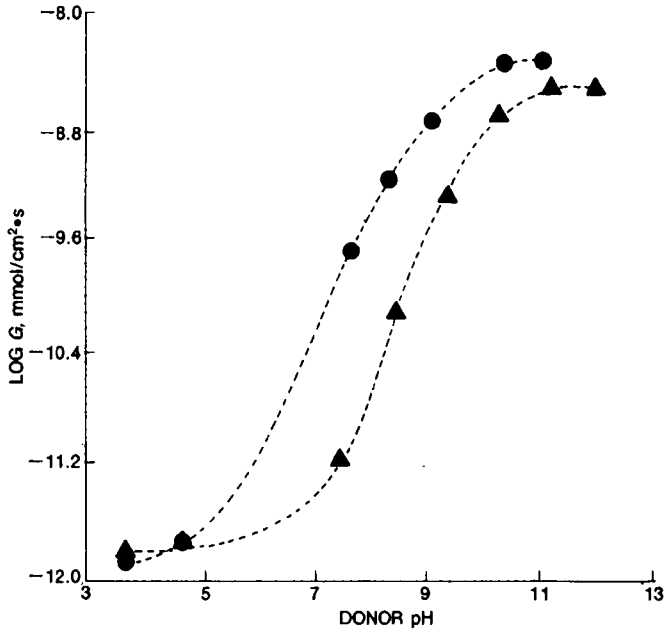

Figure 10—*Influence of chain length on flux. Assuming that the membrane diffusivities of these two compounds are approximately equal, it leads to an incremental π constant for the partition coefficient of ~0.61 per methylene group. Key: (●) octylamine; (▲) hexylamine.*

CONCLUSIONS

We have developed a rugged experimental system for studying the transport of weak acids and bases across a lipoidal membrane and developed theoretical methods for analyzing the experimental results on a quantitative basis. The experimental system consisted of the two aqueous phases separated by silicone rubber membrane. The experimental data were analyzed by utilizing theory, which takes into account the simultaneous diffusion and equilibria among all species (the various buffer species as well as the free and protonated amine), pH, and aqueous diffusion layers on both sides.

These results are conclusive evidence of the existence of aqueous diffusion barriers, as well as their effect on transport rates of solutes under varying conditions in a three-phase model. A true diffusion through the membrane of the protonated species was shown. The incremental π constant for the partition coefficient per methylene group was found to be 0.61, which is in good agreement with the value reported by Flynn and Yalkowsky (16).

Since charged bile acid micelles are not transported across the membrane, it should be possible to evaluate the degree of micellar solubilization of the amines if the study were carried out at pH 7.5–8.5, where aqueous diffusion layer effects are not important. As the un-ionized form of the amine is the major species diffusing through the membrane, the flux is the direct measurement of the thermodynamic activity of the un-ionized species and can be measured accurately, as the Donnan membrane effects encountered with cellophane membrane dialysis methods are absent.

REFERENCES

(1) R. G. Stehle and W. I. Higuchi, *J. Pharm. Sci.*, **61**, 1922 (1972).

(2) R. G. Stehle and W. I. Higuchi, *J. Pharm. Sci.*, **61**, 1931 (1972).

(3) E. R. Garrett and P. B. Chemburkar, *J. Pharm. Sci.*, **57**, 944 (1968).

(4) E. R. Garrett and P. B. Chemburkar, *J. Pharm. Sci.*, **57**, 1401 (1968).

(5) T. J. Roseman and W. I. Higuchi, *J. Pharm. Sci.*, **59**, 353 (1970).

(6) C. F. Most, *J. Appl. Polym. Sci.*, **11**, 1019 (1970).

(7) J. Haleblian, R. Runkel, N. Mueller, J. Christopherson, and K. Ng, *J. Pharm. Sci.*, **60**, 541 (1971).

(8) G. L. Flynn and T. J. Roseman, *J. Pharm. Sci.*, **60**, 1788 (1971).

(9) A. Suzuki, W. I. Higuchi, and N. F. H. Ho, *J. Pharm. Sci.*, **59**, 644 (1970).

(10) A. Suzuki, W. I. Higuchi, and N. F. H. Ho, *J. Pharm. Sci.*, **59**, 651 (1970).

(11) K. H. Kwan, W. I. Higuchi, A. M. Molokhia, and A. H. Hofmann, *J. Pharm. Sci.*, **66**, 1105 (1977).
(12) K. Gustavii and G. Schill, *Acta Pharm. Suec.*, **3**, 241 (1966).
(13) K. Gustavii, *Acta Pharm. Suec.*, **4**, 233 (1967).
(14) J. O'M. Bockris and A. K. N. Reddy, "Modern Electrochemistry," Plenum, New York, N.Y., 1970.
(15) W. I. Higuchi, S. Prakongpan, and F. Young, *J. Pharm. Sci.*, **62**, 945 (1973).
(16) G. L. Flynn and S. H. Yalkowsky, *J. Pharm. Sci.*, **61**, 838 (1972).

ACKNOWLEDGMENTS

This study was supported by Grant AM 16694 from the National Institute of Arthritis, Metabolism and Digestive Diseases.

Sintering Technique for the Preparation of Polymer Matrices for the Controlled Release of Macromolecules

JONATHAN COHEN *‡, **RONALD A. SIEGEL** §¶△, **and ROBERT LANGER** *¶‖x

Received September 13, 1982, from the *Department of Nutrition and Food Science, ‡Department of Materials Science and Engineering, §Department of Electrical Engineering and Computer Science, ¶Whitaker College of Health Sciences, Technology, and Management, Massachusetts Institute of Technology, Cambridge, MA 02139; and ‖Department of Surgery, Children's Hospital Medical Center, Boston, MA 02115. Accepted for publication July 28, 1983. △Present address: Department of Pharmaceutics, School of Pharmacy, University of California at San Francisco, San Francisco, CA 94143.

Abstract □ A new method for making polymeric systems for the controlled release of macromolecular drugs is described. The method consists of mixing drug and polymer (ethylene-vinyl acetate copolymer) powders below the glass transition temperature of the polymer and compressing the mixture at a temperature above the glass transition point. The macromolecule is not exposed to organic solvent during the fabrication process. Kinetic studies indicate that there is sustained release, and the bioactivity of macromolecules tested is unchanged throughout the sintering and release processes.

Keyphrases □ Copolymers—ethylene-vinyl acetate, controlled release of macromolecules □ Sustained release—macromolecules, ethylene-vinyl acetate copolymer □ Sintering technique—preparation of ethylene-vinyl acetate copolymer, controlled release of macromolecules

Previous studies (1, 2) have shown that controlled-release systems for macromolecules can be formulated by dissolution of ethylene-vinyl acetate copolymer in an organic solvent (dichloromethane), adding powdered macromolecule, casting the mixture in a mold at low temperature, and vacuum drying. However, the addition of solvent during the casting procedure may cause denaturation of certain macromolecules. In addition, the removal of the casting solvent in the drying step is time consuming and leads to shrinkage with possible shape distortion of the matrix. This report describes a 37°C sintering technique which takes advantage of the low glass transition temperature (−36.5°C) of ethylene-vinyl acetate copolymer and eliminates the need for solvent casting.

EXPERIMENTAL SECTION

Polymer Glass Transition Temperature—The glass transition temperature (T_g) of ethylene-vinyl acetate copolymer was determined with a differential scanning calorimeter[1] (3).

Matrix Preparation—Ethylene-vinyl acetate copolymer[2] was converted into a powder by one of two methods. The first method involved the dissolution of 3 g of ethylene-vinyl acetate copolymer in 20 mL of dichloromethane[3]. The solution was extruded dropwise, with a 50-mL syringe[4] fitted with a hypodermic needle[5], into a 250-mL beaker containing 100 mL of liquid nitrogen. From this point on, all instruments that came into contact with the frozen polymer solution were cooled with liquid nitrogen and, whenever possible, precooled in a freezer to minimize the quantity of liquid nitrogen needed for cooling.

The frozen droplets were ground for 5 min with a mortar and pestle. The powder was then spread evenly over three 20.3 × 20.3-cm glass sheets that were cooled to −10°C. The glass sheets were returned to a −10°C freezer for 2 h. At the end of that time, most of the solvent had evaporated, leaving a stringy powder. This powder was removed with a razor blade, bathed in a 100-mL beaker[6] with 30 mL of liquid nitrogen, and then ground to a fine powder with a mortar and pestle as described above. This powder was placed under vacuum for 2 h. The bulk powder was sieved to specific size ranges with a stack of graduated sieves[7]. Polymer powder prepared by this method is referred to here as powder I.

Powder I was produced under two aging conditions. In one set of experiments, the powder was dried under vacuum for 2 h at room temperature. This is referred to here as "fresh" powder I. In the other set of experiments, the powder was dried under vacuum for 2 h and then left in a covered petri dish for 1 week at room temperature. This is referred to here as "aged" powder I.

In the second method of powder preparation, 20 g of ethylene-vinyl acetate copolymer beads[2] were cooled in 40 mL of liquid nitrogen and placed in an electric mill[8]. The mill was set for 90-s grinding intervals. Between grindings, the polymer beads were cooled with 20-mL portions of liquid nitrogen. During the grinding process, cold nitrogen vapor was circulated around the sample chamber through the cooling ducts of the chamber. The powder collected around the outer edges of the sample chamber and could be extracted with a spatula after the second grinding and after every successive grinding. After the eighth grinding, ~4 g of frozen pellets was added to restore the sample to its original volume. This process was repeated until sufficient powder was collected to prepare the samples. The ground polymer powder was then sieved to specific size ranges with a stack of graduated sieves in an automatic sieve shaker[9] at −40°C. Polymer powder prepared by this second method is referred to here as powder II.

Studies were performed on both powders with either a specific particle size range (90–180 μm) or a mixture of sizes as described in Table I. To formulate the controlled-release system, macromolecular drug powder was sieved to a particle size range of 90–180 μm. Macromolecule and polymer powders, a total of 1.0 g, were placed in a plastic weighing boat[10], which was then

[1] Model DSC-II; Perkin-Elmer Corp., Norwalk, Conn.
[2] EVAc pellets, Elvax 40, prewashed to remove clay; DuPont Chemical Co., Wilmington, Del.
[3] Analytical reagent, Mallinckrodt, Inc.
[4] Becton, Dickenson and Co., Rutherford, N.J.
[5] 21-Gauge, 5.08 cm; Becton, Dickenson and Co.
[6] Pyrex; Corning Glass Works, Corning, N.Y.
[7] 450 90 μm; Newark Wire Cloth Co., Newark, N.J.
[8] Micromill model 550; Technilab Instruments, Pequannock, N.J.
[9] Portable sieve shaker; C. E. Tyler, Inc., Fisher Scientific Co., Philadelphia, Pa.
[10] Polyethylene, 75-mL capacity; VWR Scientific.

0022-3549/84/0800-1034$01.00/0